

# Mechanism of Dissolution IV: Verification of Effective Interfacial Concentration during Dissolution of a Solid

CHARLES D. SHIVELY\* and DANE O. KILDSIG<sup>▲</sup>

**Abstract** □ The effective interfacial concentration developed during dissolution was determined for five solids, ranging in solubility from 0.005 to 0.12 mole/l., using a descending column dissolution model. In all cases the interfacial concentration was evidenced by a constant concentration which developed in the first compartment of the column and was much less than saturation. The telegraph equation was used to describe the column dissolution of the solids. A second dissolution model, consisting of a round-bottom flask and a stirrer, was used to verify the effective interfacial concentrations determined in the column model. The equation, dissolution rate =  $k_i(C_s - C_i)$ , was used to analyze the data, and good agreement was obtained between the theoretical line and the experimental data, thereby verifying the values of  $C_i$ , the effective interfacial concentrations, obtained in the descending dissolution column model.

**Keyphrases** □ Dissolution of solids, descending column model—determination of effective interfacial concentration □ Interfacial concentration—determination during descending column dissolution, five solids □ Solid dissolution, descending model—determination of effective interfacial concentration □ Descending column dissolution model—effective interfacial concentration verification during solid dissolution

Recently the dissolution of a solid was studied using a column dissolution model (1). This model allowed dissolution to be studied under both ascending and descending conditions. For dissolution in the ascending model, excellent agreement was obtained between the experimental amount dissolved and the concentrations predicted by Fick's second law. In the descending model, a mathematical model involving an autocorrelation step was required to describe the observed experimental concentration gradient. It was in the descending model that an interfacial concentration, much less than saturation, was determined.

This report describes the determination of the effective interfacial concentration for additional solids in the column dissolution model and provides verification of the effective interfacial concentrations by a completely different dissolution model.

## GENERAL CONSIDERATIONS

The concentration of solute that developed in the compartment adjacent to the solid surface in the dissolution column described in the previous report (1) was found to reach a constant value during dissolution. This concentration was taken to be the effective interfacial concentration existing at the solid-liquid interface for an interfacially controlled dissolution process. The theoretical concentration gradient predicted by the telegraph equation (1) using this effective interfacial concentration was in good agreement with the experimental concentration gradient developed in the descending column model. However, since only one solid was used in the initial investigation, it was possible that the development of an equilibrium concentration in the first compartment was peculiar to that solid. Furthermore, it was entirely possible that the equilibrium concentration developed in the first compartment during descending dissolution was entirely dependent upon the column model and not related to the solid itself.

Table I—Diffusion Coefficients at 30°

Solute	Concentration, g. ml. <sup>-1</sup> × 10 <sup>3</sup>	Diffusion Coefficient, cm. <sup>2</sup> sec. <sup>-1</sup> × 10 <sup>5</sup>
Phenacetin	0.000	0.900 <sup>a</sup>
	0.179	0.895
	0.364	0.894
	0.538	0.862
	0.717	0.857
	0.896	0.860
Salicylamide	0.000	1.41 <sup>a</sup>
	0.137	1.37
	0.343	1.30
	0.686	1.21
	1.029	1.15
	1.371	1.14
	2.057	1.11
2.469	1.08	
<i>m</i> -Acetotoluide	0.000	1.25 <sup>a</sup>
	0.149	1.22
	0.746	1.15
	1.490	1.12
	2.238	1.08
	3.730	1.07
	5.968	1.06
Benzamide	0.000	1.16 <sup>a</sup>
	0.121	1.15
	0.621	1.13
	1.211	1.11
	6.055	1.08
	12.114	1.07
14.750	1.07	

<sup>a</sup> Obtained by extrapolation to infinite dilution.

With these two possibilities in mind, it was decided to investigate the dissolution properties of several additional solids using the column dissolution model and, in addition, to use a dissolution model significantly different from the column model. A mathematical model was chosen which had previously been utilized in describing an apparent interfacially controlled dissolution process (2):

$$\text{dissolution rate} = k_i(C_s - C_i) \quad (\text{Eq. 1})$$

where  $k_i$  is the interfacial rate constant,  $C_s$  is the saturation solubility, and  $C_i$  is the effective interfacial concentration. This model relates the dissolution rate to the driving force for dissolution,  $C_s - C_i$ . From Eq. 1, it can be seen that if  $C_s$  were decreased for a given solid, such as by the addition of a neutral salt to the dissolution medium, the dissolution rate should approach zero as  $C_s$  approaches  $C_i$  and it should be possible to predict  $C_i$  from a plot of dissolution rate versus  $C_s$ . If  $C_i$  is dependent only on the nature of the solid, this graphical approach to the determination of  $C_i$  should be independent of the dissolution model itself and of the degree of agitation in the dissolution model. For this reason, a round-bottom flask with provision for agitation was chosen as the dissolution model to be used in comparison with the column dissolution model.

## EXPERIMENTAL

**Materials**—The materials used in this study were benzamide<sup>1</sup>, *m*-hydroxybenzoic acid<sup>1</sup>, *m*-acetotoluide<sup>1</sup>, 2,5-dihydroxybenzoic acid<sup>1</sup>, salicylamide NF, and phenacetin USP. All chemicals were used

<sup>1</sup> Eastman reagent chemicals.

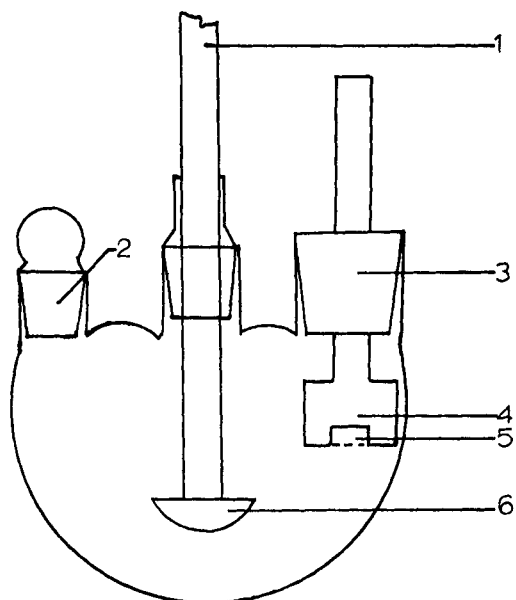


Figure 1—Vessel dissolution model. Key: 1, glass stirrer shaft; 2, ground-glass stopper; 3, holder for die-tablet assembly; 4, tablet holder; 5, fused tablet disk; and 6, stirring paddle.

as received from the manufacturer. The water used in the dissolution media was double distilled, the second time in an all-glass still.

**Diffusion Cell**—The basic diffusion cell used in this study was a replica of that described by Nedich and Kildsig (1), with the exception that a 3.7-cm. diameter nylon reinforced filter (M.F. Millipore, microweb) with a 4- $\mu$  pore size was used as the diffusion membrane instead of the silver membrane. The nylon membrane did not require any special pretreatment prior to use in the diffusion coefficient determinations (3) and eliminated the oxidation problem associated with the silver membrane.

The two-flask diffusion cell was held together by an aluminum clamp secured by four nuts and bolts. This clamp was placed over the ground-glass joints and, following assemblage of the cell, the joint area was coated with paraffin to ensure a leak-free seal.

Solutions placed in these flasks were stirred at 450 r.p.m. by the use of magnetic stirrers and 5-cm. Teflon-coated magnetic stirrer bars. The 450-r.p.m. speed was maintained constant by monitoring<sup>2</sup> the speed of the stirrer bars. The diffusion cell was then placed in a water bath maintained at  $30 \pm 0.02^\circ$ .

The cell constant was determined using potassium chloride as the diffusing solute. The cell was filled and placed in the water bath at  $30^\circ$ , and a 4-hr. lag time was used before the first sample, time = zero, was removed. Samples of 10-ml. volume were subsequently removed at 30-min. intervals for 2.5- or 3-hr. periods. The volume withdrawn was replaced after each sample, and corrections were made for the potassium chloride concentration withdrawn. An atomic absorption spectrophotometer<sup>3</sup> was used to assay the potassium ion

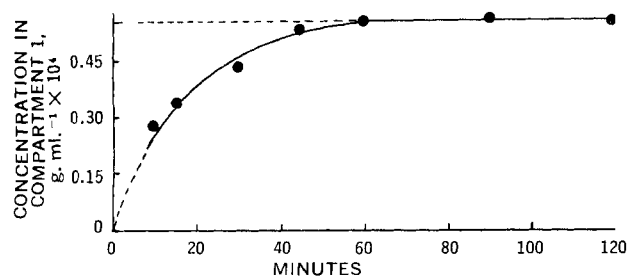


Figure 2—Phenacetin concentration in Compartment 1 as a function of time obtained in the descending column model. The plateau value is the effective interfacial concentration,  $C_i$ .

Table II—Comparison of Amount Dissolved in Ascending Compartmental Model Dissolution

Solute	Hours	Theoretical Concentration, g. $\times 10^3$	Experimental Concentration, g. $\times 10^3$	Percent Deviation
Benzamide	6	8.196	7.824	-4.54
<i>m</i> -Acetoluide	25	6.595	6.605	+0.15
Salicylamide	30	3.345	3.253	-2.75
Phenacetin	8	0.517	0.516	-0.19

present in each solution, and the concentration was adjusted for potassium chloride content. The concentration of the potassium chloride solution in the initial flask was determined before and after each experimental run to ensure that the equilibrium plateau of the diffusion curve had not been reached. The diffusion coefficient of a 0.1 M KCl solution was taken as  $2.0934 \times 10^{-5}$  cm.<sup>2</sup>/sec. (4) for calculation of the cell constant. The diffusion coefficients of several solids at varying solute concentration are shown in Table I.

**Solid Disk Preparation**—The solid disks used in this study were all prepared by the same method. Each individual disk was formed by first melting the solid in a casserole. The melt was then poured onto a highly polished stainless steel punch inserted into a die. The punch and die assembly was brought to within  $10^\circ$  of the melting point of the solid prior to tablet formation. After pouring the solid melt into the punch and die assembly, a cylindrical glass vessel was placed over the entire assembly and the solid was allowed to fuse. The temperature of the punch and die assembly including the newly fused tablet was allowed to cool to room temperature, and the newly formed solid disk was removed. The uniformity of the fused disks was evidenced by the good tablet to tablet reproducibility of dissolution rates.

**Determination of Saturation Solubility of Solids in Various Solvents**—The solubility of the six solids in various solvents was determined at  $30^\circ$  using a three-necked, 100-ml., round-bottom flask submerged in a water bath. Excess solid material was placed in 100 ml. of the respective solvent (either doubly distilled water or 0.1, 0.25, 0.50, or 1.0 M NaCl aqueous solutions) and stirred for 4 days. Two-milliliter samples were removed every 24 hr. using a warmed Millipore filter syringe with a filter pore size of 0.65 or 0.45  $\mu$ , diluted where necessary, and assayed spectrophotometrically.

**Compartmental Dissolution Model**—The compartmental dissolution column, consisting of a series of 14 Plexiglas compartments, each 3 cm. in height and containing a volume of 2.89 ml., was described previously (1), as was the environmental chamber for maintaining column temperature at  $30 \pm 0.01^\circ$  (1). A 2-hr. equilibrium period within the chamber was allowed following positioning of the filled column. This 2-hr. equilibrium allowed the system to attain both temperature equilibrium and static fluid equilibrium inside the column. Ascending dissolution or descending dissolution dictated the position of the tablet-containing slide at the bottom or top of the column, respectively. After the equilibrium period, the tablet was positioned either under or on top of the column of solvent and dissolution was allowed to occur. Following a definite time period of dissolution, the tablet-containing slide was moved out of position and the compartments were closed by moving the draw-rod and slides into the closed position.

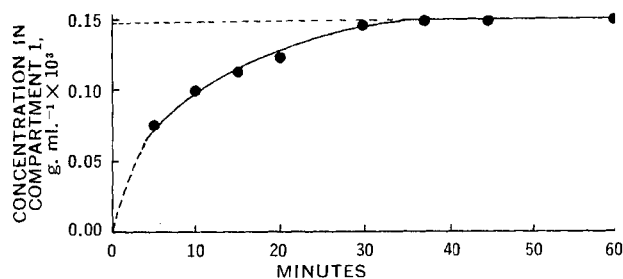


Figure 3—Salicylamide concentration in Compartment 1 as a function of time obtained in the descending column model. The plateau value is the effective interfacial concentration,  $C_i$ .

<sup>2</sup> With a Strobotac unit, General Radio Corp., Concord, Mass.

<sup>3</sup> Model 290, Perkin-Elmer Corp., Norwalk, Conn.

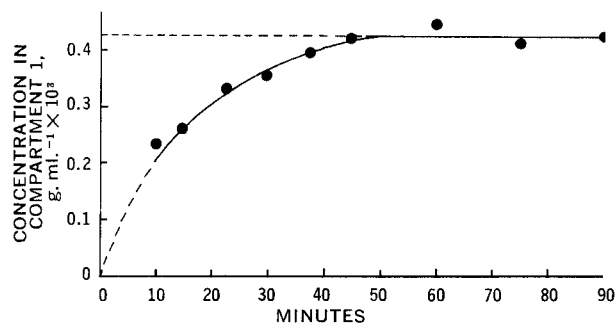


Figure 4—*m*-Acetotoluide concentration in Compartment 1 as a function of time obtained in the descending column model. The plateau value is the effective interfacial concentration,  $C_i$ .

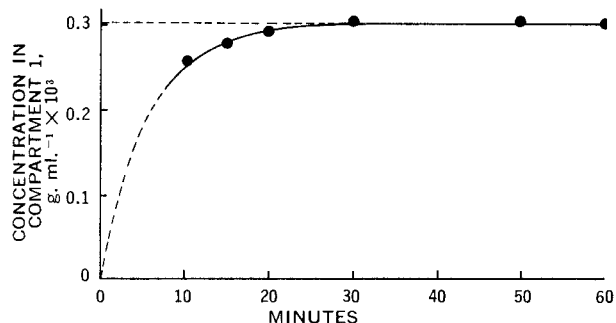


Figure 5—*m*-Hydroxybenzoic acid concentration in Compartment 1 as a function of time obtained in the descending column model. The plateau value is the effective interfacial concentration,  $C_i$ .

The column was removed from its support in the oven and the samples were withdrawn using the 5-ml. syringes. Following proper dilution, the contents were assayed spectrophotometrically.

Experimental results from ascending dissolution studies were compared to concentrations predicted by Fick's second diffusion law with a concentration-dependent diffusion coefficient using the solution to Fick's equation as previously reported (1). Experimental results from descending dissolution studies were compared to the concentration gradient predicted by the telegraph equation using the appropriate initial and boundary conditions (1). All data relevant to ascending and descending dissolution studies were analyzed on a computer<sup>4</sup>.

**Vessel Dissolution Model**—The vessel dissolution model (Fig. 1) was a three-necked, 1000-ml., round-bottom flask modified to accept a stirrer and a Plexiglas die containing a fused tablet. Agitation of the dissolution medium was achieved by a stirrer mounted vertically through the center of the flask. The stirrer consisted of a 0.93-cm. (0.38-in.) glass shaft with a half-oval-shaped paddle of dimen-

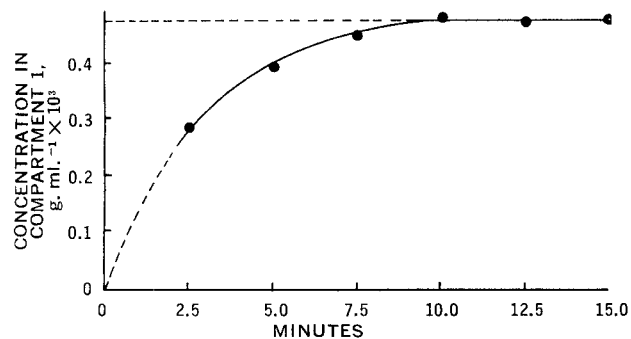


Figure 6—Benzamide concentration in Compartment 1 as a function of time obtained in the descending column model. The plateau value is the effective interfacial concentration,  $C_i$ .

Table III—Effective Interfacial Concentrations Determined in the Descending Column Model

Solid	Saturation Solubility, $C_s$ , moles/l. $\times 10^2$	Interfacial Concentration, $C_i$ , moles/l. $\times 10^3$
Phenacetin	0.53	0.32
Salicylamide	2.0	1.1
<i>m</i> -Acetotoluide	4.1	2.8
<i>m</i> -Hydroxybenzoic acid	7.6	2.6
Benzamide	12.5	4.0
2,5-Dihydroxybenzoic acid	18.0	3.6

sions  $2.5 \times 7.0$  cm. attached to a stirrer motor<sup>5</sup>. The stirrer paddle was immersed to within 3.0 cm. of the bottom of the vessel. The vessel was filled with 500 ml. of the solvent and the assembly, without the die, was lowered into a water bath maintained at  $30^\circ$ . The fused solid, placed in the die, was then lowered into the vessel and immersed 1 cm. below the surface of the solvent. The dissolution of the solids was conducted under static conditions and 50- and 100-r.p.m. stirred conditions in doubly distilled water and 0.1, 0.25, 0.50, and 1.0 *M* NaCl aqueous solutions. Dissolution was allowed to proceed for 5- or 10-min. intervals, depending upon the solid under investigation, and then the die-tablet was removed and blotted dry. The solution was then stirred at 450 r.p.m. for 1 min. A 2- or 5-ml. sample was then removed and diluted where necessary prior to spectrophotometric assay. The solution in the vessel was allowed to become static and the die-tablet was replaced. Dissolution was then allowed to occur for another 5- or 10-min. period. This procedure was carried out for a total of 1 hr. dissolution time for each solid in each solvent.

## RESULTS AND DISCUSSION

**Ascending Column Dissolution**—Since an extensive study concerning the conditions and use of Fick's second diffusion law to predict the concentration profile as a function of time and distance has been

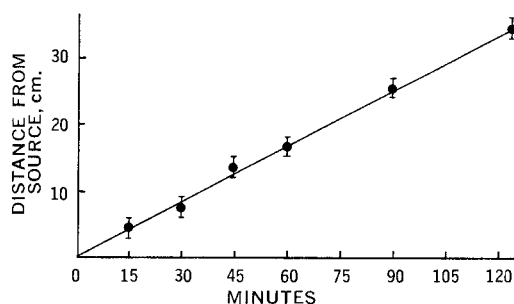


Figure 7—Relationship between the distance of the phenacetin solute front from the tablet source and dissolution time in the descending column. The indicated limits are the geometrical limits of the length of the column compartments and are not statistical limits.

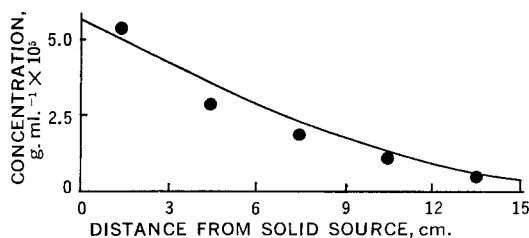


Figure 8—Comparison of theoretical (—) and experimental (●) concentration gradients for phenacetin descending dissolution at the end of 45 min. The theoretical concentration is that predicted by the telegraph equation (1).

<sup>4</sup> CDC 6500, at the computer center of Purdue University.

<sup>5</sup> Stedi-Speed Adjustable Stirrer, Fisher Scientific Co., Chicago, Ill.

**Table IV**—Velocity of the Solute Front Passing down the Dissolution Column

Solute	Velocity, cm. sec. <sup>-1</sup> × 10 <sup>2</sup>
Phenacetin	0.478
Salicylamide	1.596
<i>m</i> -Acetotoluide	1.267
Benzamide	4.166

completed (1), validation of diffusion control in the ascending column model was sought for only one time period for several solids.

The solution concentration at any point in the dissolution column depends upon which of the rate processes, the interfacial rate or the diffusion rate, is faster. When the interfacial reaction rate is fast compared to the diffusional rate, the experimentally determined concentration would equal the theoretical concentration as predicted by the presence of a saturated layer. If the interfacial rate is slow compared to the rate of diffusion, the experimentally determined concentration obtained would be much less than the theoretical concentration predicted on the basis of a saturated layer model.

A comparison of the theoretically predicted amount dissolved using Fick's second law and the experimental amount dissolved for benzamide, salicylamide, phenacetin, and *m*-acetotoluide is shown in Table II for various dissolution time periods. This excellent agreement shows that under ascending model conditions the dissolution process is diffusion controlled and mathematically described by Fick's second law of unidimensional diffusion. As diffusion control of this model is apparent, the mass transfer step of the dissolution process is the controlling factor.

**Descending Column Dissolution**—In the descending model, the solid surface and solid-liquid interface are at the top of the liquid column and the solute moves in a downward direction following dissolution. It was anticipated that the mass transfer step would be fast in relation to the solid-liquid interaction or solvation rate. The solute concentration in the first compartment adjacent to the solid surface verifies the slow interfacial reaction rate because it is far less than saturation and attains a plateau value with increasing dissolution time periods for each solid studied (Figs. 2-6). This concentration, less than saturation, is apparently in equilibrium with the solid

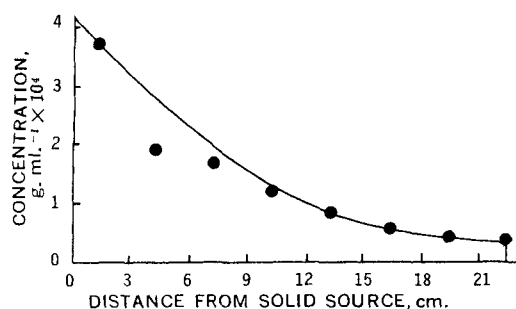


**Figure 9**—Comparison of theoretical (—) and experimental (●) concentration gradients for *m*-acetotoluide descending dissolution at the end of 30 min. The theoretical concentration is that predicted by the telegraph equation (1).

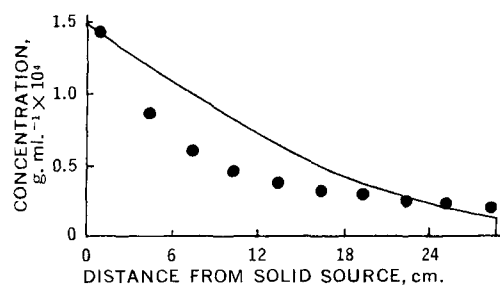


**Figure 10**—Comparison of theoretical (—) and experimental (●) concentration gradients for salicylamide descending dissolution at the end of 30 min. The theoretical concentration is that predicted by the telegraph equation (1).

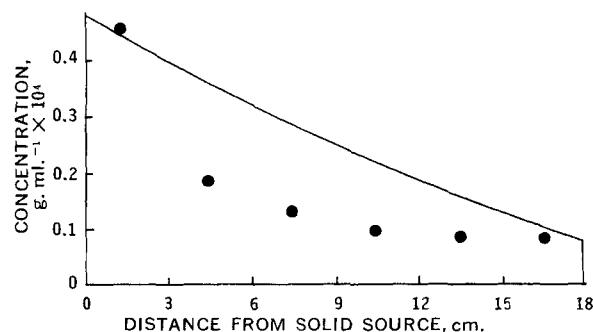


**Figure 11**—Comparison of theoretical (—) and experimental (●) concentration gradients for benzamide descending dissolution at the end of 7.5 min. The theoretical concentration is that predicted by the telegraph equation (1).

surface and is interpreted as being the effective concentration existing at the solid-liquid interface. In addition, it represents the effective concentration available to the bulk solution at this interface (Table III).

The development of an equilibrium concentration in the first compartment during descending dissolution is obviously not associated solely with the original solid studied, *m*-acetotoluide (1). Instead, Figs. 2-6 clearly show that, in addition to *m*-acetotoluide, an equilibrium concentration is obtained for each solid, the magnitude of which varies from solid to solid. It would appear from this that the equilibrium concentration developed in the first compartment, which was previously equated to the effective interfacial concentration, is dependent on the nature of the dissolving solid. It will be shown below, when using the vessel dissolution model, that assuming the equilibrium concentration in the first compartment of the descending model to be equal to the effective interfacial concentration of solute,  $C_i$ , is justified.

The concentration gradients developed in the descending column model reveal a rather abrupt drop in solute concentration at some time-dependent distance from the tablet source for all solids studied. This was observed previously for *m*-acetotoluide (1). If the distance at which this abrupt drop in concentration occurs is plotted as a function of time, a linear relationship can be seen. The slope of this graph is the velocity of flow of the solute front from the solid-liquid interface into the bulk of the dissolution medium (Fig. 7). The limits presented in Fig. 7 are the geometrical limits involved with the length of the compartment and are not statistical limits. Velocity values for several of the solids investigated were determined in this manner and are presented in Table IV.

The descending column model represents a physical system where two miscible liquids are in contact. These two miscible liquids are the solvated solute solution and the pure bulk solution. When the solvated or hydrated solute molecules flow through the stationary liquid solvent, the fluid elements or holes comprising the liquid solvent can act as a channeling or dispersion medium. The ability of the liquid solvent to channel or disperse the hydrated solute as the hydrated solute passes down the column may be considered analogous to the flow of a liquid through a porous bed of solid material.

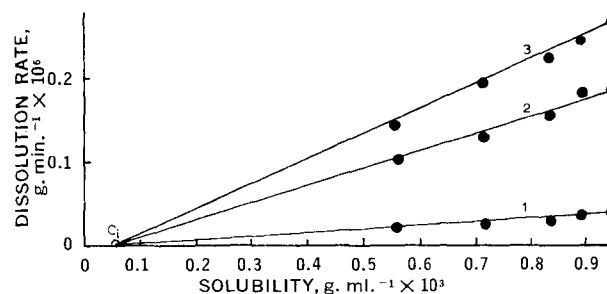


**Figure 12**—Comparison of theoretical (—) and experimental (●) dissolution rates of phenacetin as a function of solubility,  $C_s$ . The theoretical line is that predicted by Eq. 1 using the value of  $C_i$  determined by the column dissolution model. Key: 1, 0 r.p.m.; 2, 50 r.p.m.; and 3, 100 r.p.m.

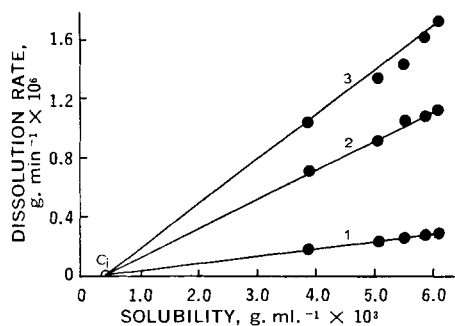


**Figure 13**—Comparison of theoretical (—) and experimental (●) dissolution rates of *m*-acetotoluide as a function of solubility,  $C_s$ . The theoretical line is that predicted by Eq. 1 using the value of  $C_i$  determined by the column dissolution model. Key: 1, 0 r.p.m.; 2, 50 r.p.m.; and 3, 100 r.p.m.

Previous utilization (1) of the random-walk model with autocorrelation for a flow-through porous medium as applied to the descending method gave encouraging results. Application of the random-walk model with autocorrelation is consistent with the physical phenomena that occur during descending column dissolution. The abrupt drop in solute concentration at some time-dependent distance from the solid surface strongly suggests a solute front traveling through the medium with a finite velocity. In addition, as the miscible hydrated solute front passes through the liquid medium, it mixes and is dispersed among the liquid elements. The random-walk model with autocorrelation does not involve the asymptotical approach to zero concentration inherent in the solution of the diffusion equation but rather predicts a solute front with finite concentration as a function of distance and time.

A comparison of the concentration profiles predicted by the telegraph equation and the experimentally determined profiles are shown for a representative time period for four solids (Figs. 8–11), illustrating the most accurate (Figs. 8 and 9) and least accurate (Figs. 10 and 11) fit of the data.

The precision with which the random-walk model with autocorrelation fits the descending column model is apparently dependent on the nature of the solute. An extremely accurate fit was obtained for phenacetin (Fig. 8), while deviations were observed for benzamide (Fig. 11). Deviations of this type are to be expected, however, due to the nature of a flow-through porous medium which is dependent on the microdynamics of fluid flow-through channels in the porous medium. Consequently, this deviation from the theoretically predicted curves may be a result of the hydrated solute state of the solids, the hydrodynamics of the flowing solute front, or the nature of the stationary dispersion medium.

Since the velocity determination of the solute front passing through the column is made experimentally and used in the prediction of the theoretical curve, the apparent abrupt drop in concentration observed in the column may not represent the true position of the distinct solute front. It is possible in certain cases that the solvated solute moves faster in the center of the column than it does near the column wall. This phenomenon is observed in many cases of flow-through horizontal cylinders and results in the establishment of an elongated parabolic solute front.

If this phenomenon were to occur, it would be expected for those solids that pass quickly through the column and are not adequately dispersed to form a distinct solute front. In such cases, radial diffusion of the solute is slow compared to the velocity component of solute flow. When the solvated solute passes through the column at a slower velocity, the effect of radial diffusion should be more apparent and there should be greater dispersion from the center of the column to the walls of the column. This would predict a more distinct demarcation line between the solute front flowing down the column and the stationary liquid medium in the column.

In addition, a nonuniform density distribution of the flowing solvated solute, when combined with gravitational forces, could cause

**Table V**—Correlation Coefficients for Experimental Verification of Eq. 1 Using Vessel Dissolution Model

Solid	Agitation Conditions		
	Static	50 r.p.m.	100 r.p.m.
Phenacetin	0.970	0.994	0.998
Salicylamide	0.995	0.996	0.996
<i>m</i> -Acetotoluide	0.998	0.998	0.995
Benzamide	0.988	0.992	0.996

the higher density solvated solute particles to flow through the medium at a greater rate than less dense solvated solute. It is difficult to determine the effect of density differences in descending dissolution, since no significant difference appears to exist between solution densities of the solutes corresponding to the effective concentration at the solid-liquid interface. However, the solution densities were determined by the pycnometer method, which may lack sufficient accuracy to delineate the true dependence of solute flow on the density differences arising from changing concentration gradients.

**Vessel Dissolution Model**—Equation 1 predicts that the dissolution rate should approach zero as  $C_s$  approaches  $C_i$  for an interfacially controlled dissolution process. If the effective interfacial concentration,  $C_i$ , is a characteristic of the solid under interfacially controlled conditions, it should remain essentially constant during the dissolution process regardless of agitation conditions. This is also true for the saturation solubility  $C_s$ .

With  $C_s$  and  $C_i$  constant, a theoretical line describing the dissolution rate-solubility relationship can be drawn from Eq. 1 utilizing a dissolution rate versus solubility ( $C_s$ ) graph. This line can be drawn using the dissolution rate of the solid in pure water and, using the value of  $C_i$  from the column model, the zero dissolution rate predicted by Eq. 1 when  $C_s = C_i$ . The dissolution rates of the solid, as a function of decreasing solubility of the solid, should then fall along this theoretical line.

To test the validity of this hypothesis, the dissolution rates of several solids from fused disks were determined under conditions of 0-, 50-, and 100-r.p.m. agitation in a round-bottom flask and, using the dissolution rate versus  $C_s$  relationship described above, the experimental data were compared with the theoretical line predicted by Eq. 1. The results are shown in Figs. 12 and 13. Similar results were obtained for *m*-acetotoluide and salicylamide.

Table V shows the correlation coefficients for the data in Figs. 12 and 13. It is obvious that excellent agreement exists between the mathematical model (Eq. 1) and the experimental data. The concept of an effective interfacial concentration at the solid-liquid interface that is less than saturation has, therefore, been experimentally confirmed for several solids having solubilities ranging from 0.005 to 0.120 mole/l.

## REFERENCES

- (1) R. L. Nedich and D. O. Kildsig, *J. Pharm. Sci.*, **61**, 214 (1972).
- (2) D. E. Wurster and D. O. Kildsig, *ibid.*, **54**, 1491 (1965).
- (3) G. G. Smith, Ph.D. thesis, Purdue University, Lafayette, Ind., 1970.
- (4) H. S. Harned and R. L. Nuttall, *Ann. N. Y. Acad. Sci.*, **46**, 285 (1945).
- (5) C. B. King and M. M. Braverman, *J. Amer. Chem. Soc.*, **54**, 1744 (1932).

## ACKNOWLEDGMENTS AND ADDRESSES

Received March 23, 1972, from the Department of Industrial and Physical Pharmacy, School of Pharmacy and Pharmaceutical Sciences, Purdue University, Lafayette, IN 47907

Accepted for publication May 25, 1972.

\* American Foundation for Pharmaceutical Education Fellow. Present address: Alcon Laboratories, Ft. Worth, Tex.

▲ To whom inquiries should be directed.